

Relativistic Radiation Belt Electron Responses to GEM Magnetic Storms :Comparison of CRRES Observations with 3-D VERB simulations

**Kyung-Chan Kim¹, Yuri Shprits^{2,3,4}
Dmitriy Subbotin⁴, Binbin Ni⁴**

¹Korea Astronomy and Space Science Institute, Korea

²Institute of Geophysics and Planetary Physics, UCLA

³Dept. of Earth and Space Sciences, UCLA

⁴Dept. of Atmospheric and Oceanic Sciences, UCLA

- **Goals here**

- The U.S. National Science Foundation's Geospace Environment Modeling (GEM) has identified for detailed case study five magnetic storms that occurred during the second half of the Combined Release and Radiation Effects Satellite (CRRES) mission in the year 1991.
- Show the responses of relativistic radiation belt electrons to these storms by comparing the time-dependent 3-D Versatile Electron Radiation Belt (VERB) simulations with the CRRES MEA 1 MeV electron observations
- Investigate the relative roles of competing effects of the previously proposed scattering mechanisms at different storm phases, as well as examine the extent to which the simulation efficiently represents the observation.

• Fokker-Plank diffusion equation

$$\begin{aligned} \frac{\partial f}{\partial t} = & L^{*2} \frac{\partial}{\partial L^*} \bigg|_{\mu,J} \left(D_{L^*L^*} L^{*-2} \frac{\partial f}{\partial L^*} \bigg|_{\mu,J} \right) \\ & + \frac{1}{T(y)y} \frac{\partial}{\partial y} \bigg|_{p,L^*} \left(T(y)y \langle D_{yy} \rangle \frac{\partial f}{\partial y} \bigg|_{p,L^*} + T(y)y \langle D_{yp} \rangle \frac{\partial f}{\partial p} \bigg|_{y,L^*} \right) \\ & + \frac{1}{p^2} \frac{\partial}{\partial p} \bigg|_{y,L^*} \left(p^2 \langle D_{pp} \rangle \frac{\partial f}{\partial p} \bigg|_{y,L^*} + p^2 \langle D_{py} \rangle \frac{\partial f}{\partial y} \bigg|_{p,L^*} \right) \\ & + \text{Source} - \text{Loss} \end{aligned}$$

- Recently developed time-dependent [Versatile Electron Radiation Belt \(VERB\) code](#) [see *Shprits et al., 2008*; *Subbotin and Shprits, 2009*; *Kim et al., 2011* for more details]

• Simulation Methodology

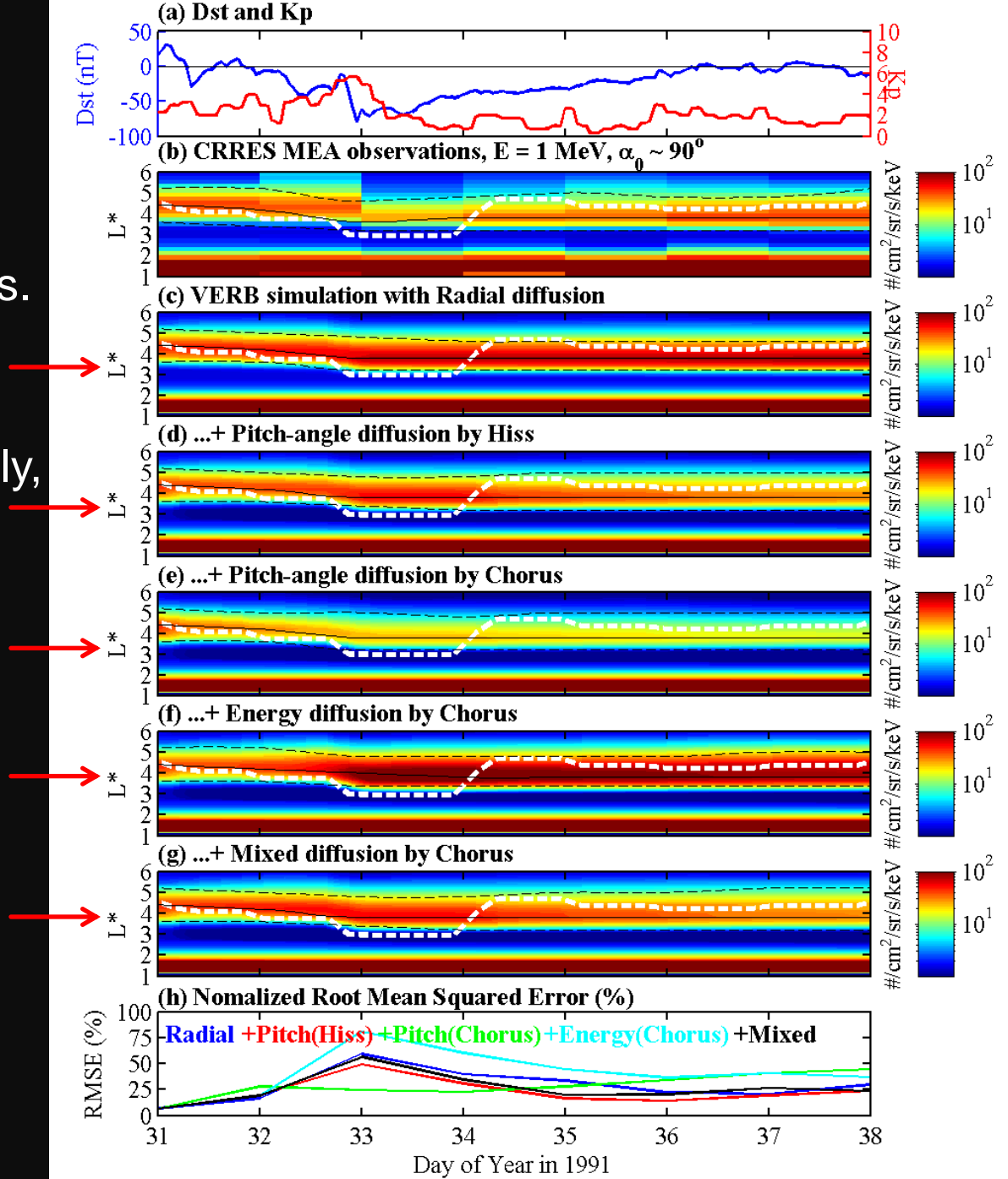
- Radial diffusion by ULF electromagnetic fluctuations

$$D_{L^*L^*}^M(Kp, L^*) = 10^{(0.506Kp - 9.325)} L^{*10} \quad (Kp = 1 \text{ to } 6) \quad [\text{Brautigam and Albert, 2000}]$$

- Outside the plasmopause, pitch-angle scattering and local acceleration by **day-night chorus waves** including mixed diffusion
- Inside the plasmopause, pitch-angle diffusion by **plasmaspheric hiss**
- **Plasmopause motion** in response to the Kp variation
- **Flux variation at outer boundary** ($L^*=6.6$), taken from the CRRES MEA observations of 1 MeV electron fluxes

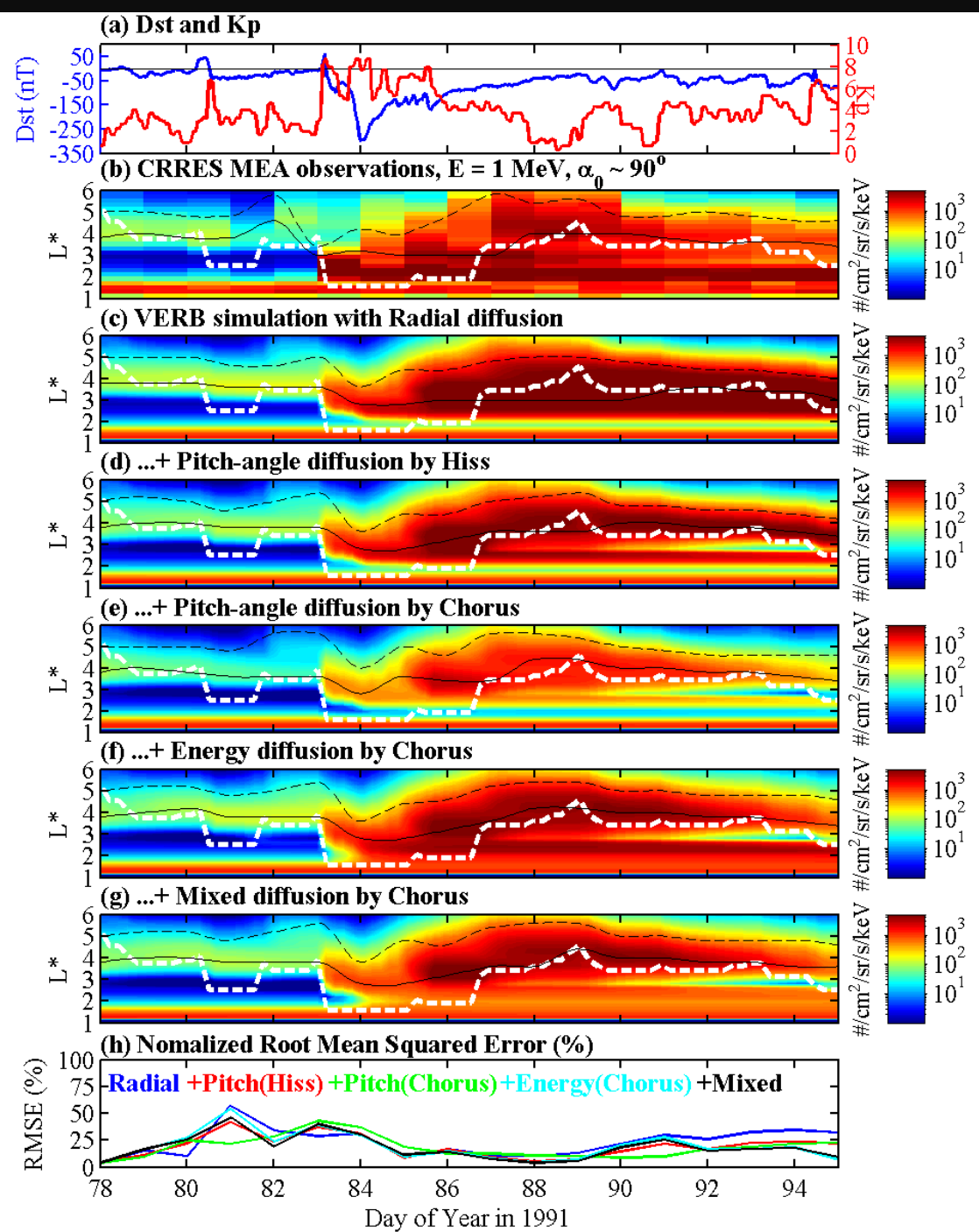
February Storm, 1991

- Peak fluxes diffuse inward during main phase, then during recovery increase gradually, diffusing outwards.
 - inward diffusion and further enhancement
 - flux decrease gradually, injected into the plasmasphere
 - further decrease
- overestimated fluxes
- reduce enhanced fluxes



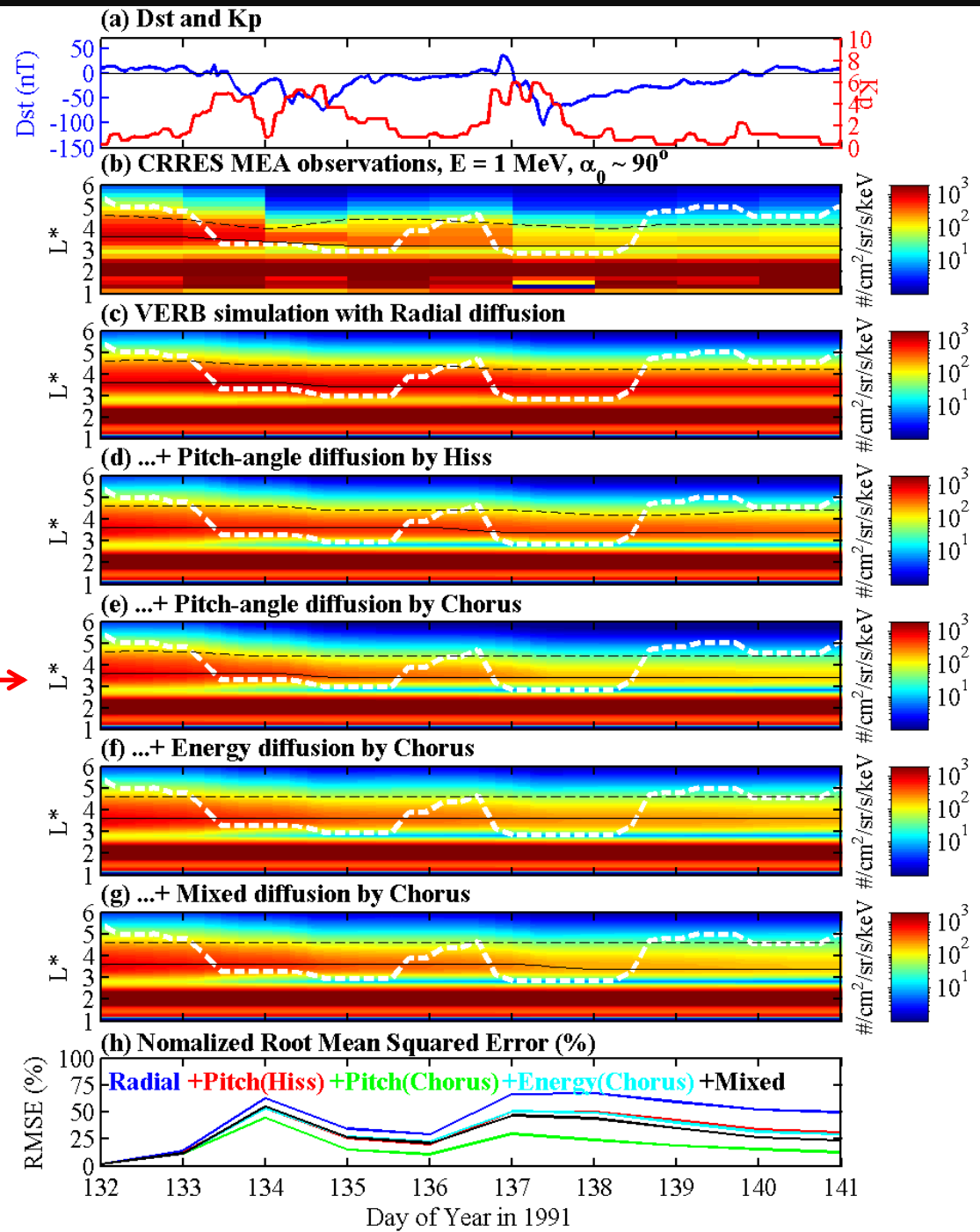
March Storm, 1991

- Proton contamination initiated by the 24 March (day 82) prompt injection
- Simulation shows a new radiation belt ($2 < L^* < 3$):
 - initiated by either continuous inward radial transport into $L^* = 2$ or local acceleration
 - undergoes a slow decay inside the plasmapause by plasmaspheric hiss



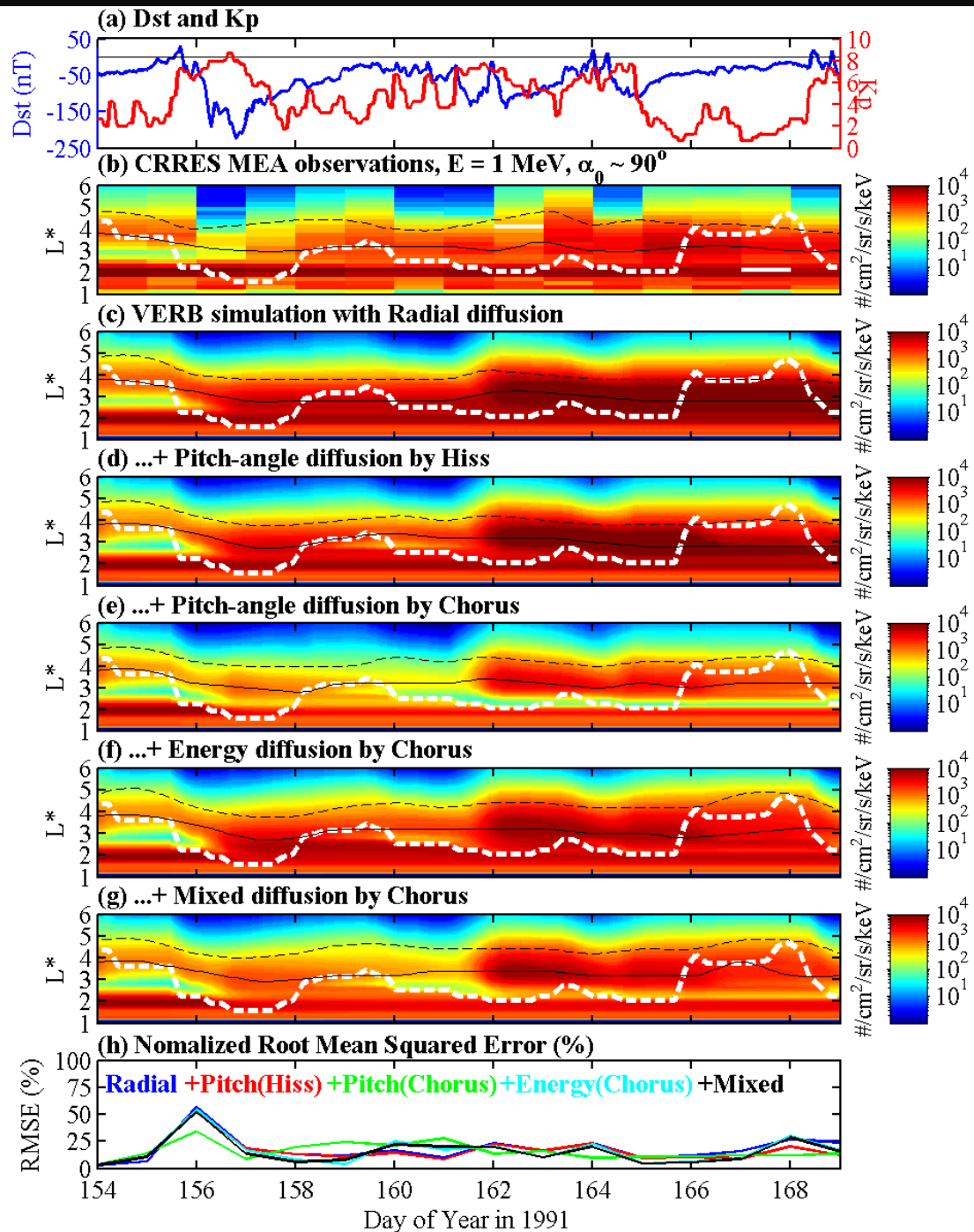
May Storm, 1991

- CRRES observations show every time Dst fully recovers the peak flux level decreases by approximately half an order of magnitude relative to its pre-storm level
- Pitch-angle scattering by chorus waves outside of the plasmopause largely account for such a post-storm flux level



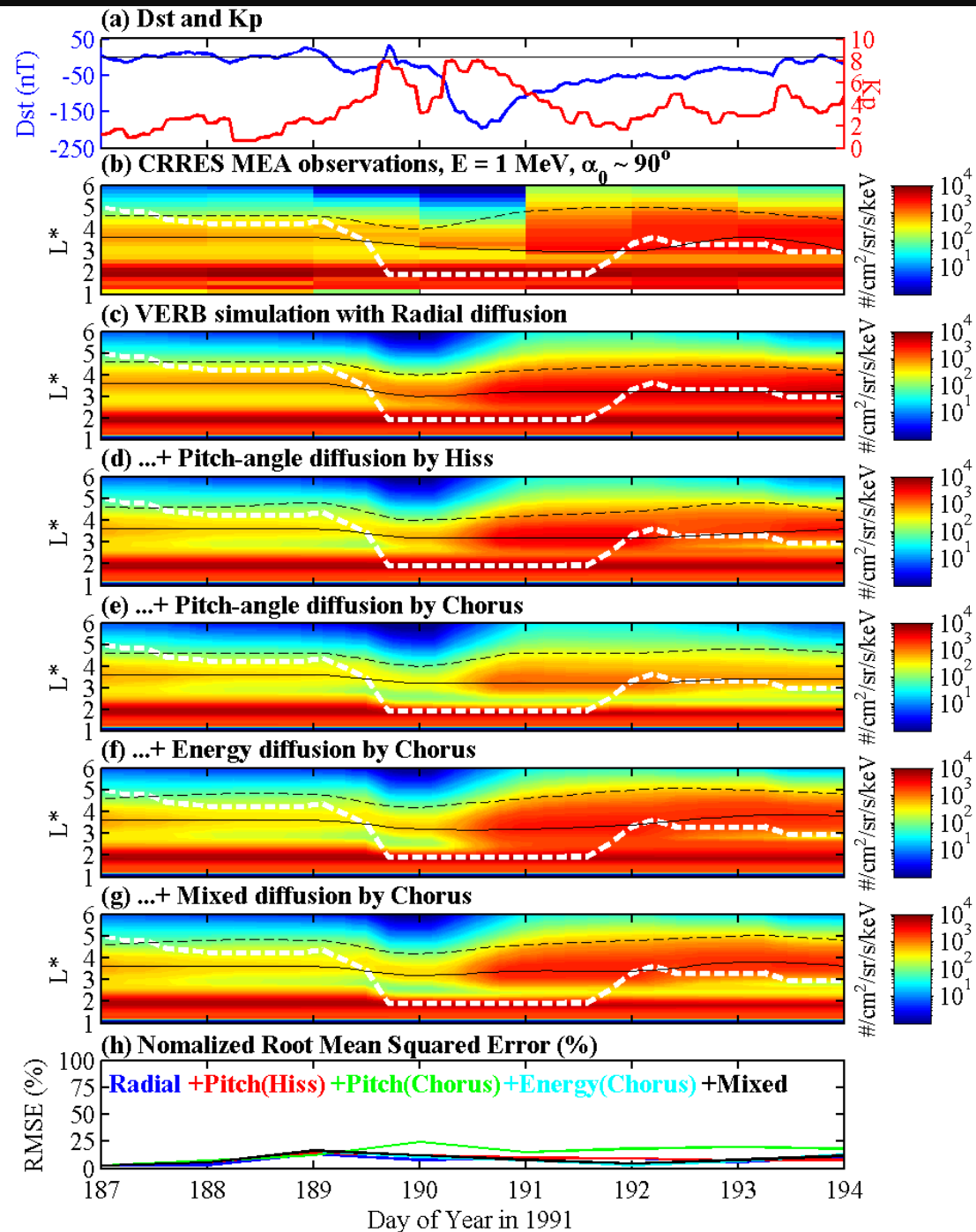
June Storm, 1991 : a tripe-Dst dip storm

- Both measured and predicted fluxes diffuse inward during the main phase of each of the storm's multiple dips, and during the recovery phase of the first two dips and the early recovery of the last dip the diffusion takes place in outward direction



July Storm, 1991

- During the early recovery, measured flux starts to increase substantially and even exceed its pre-storm level
- Simulation also predicts such flux buildups, which could be accounted for by inward radial diffusion only or local acceleration

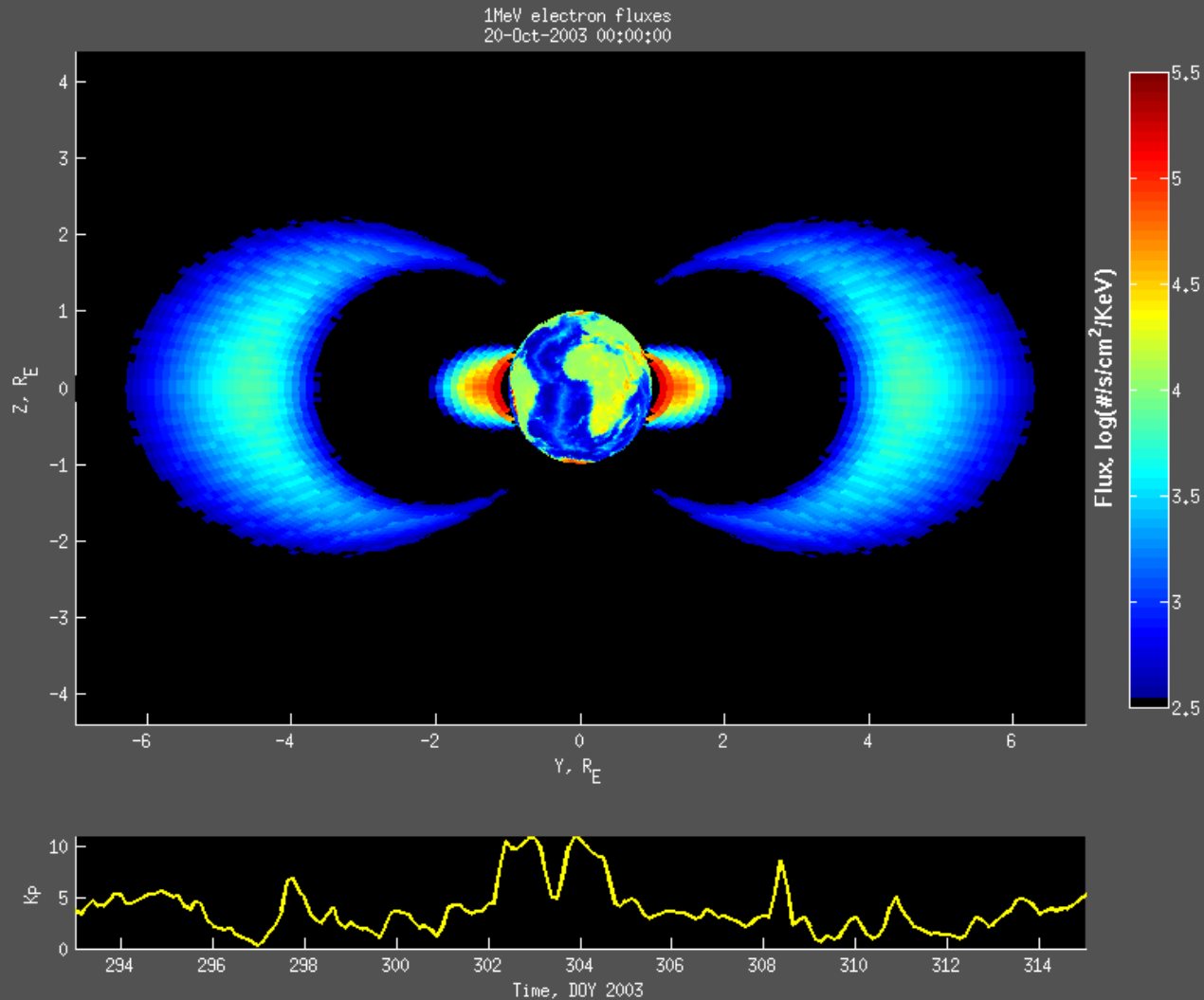


Event	Mechanism	Inner edge	Outer edge	Location of outer belt flux peak	$\langle \text{RMSE}/\text{obs}_{\text{mean}} \rangle$
1991/February Extended recovery	Radial	0.96	0.56	0.96	28.6
	+ Pitch-angle (Hiss)	0.88	0.75	0.96	22.5
	+ Pitch-angle (Chorus)	0.96	0.52	0.96	28.5
	+ Energy (Chorus)	0.96	0.78	0.82	40.6
	+ Mixed (Chorus)	0.88	0.53	0.96	25.9
1991/March Superstorm interval	Radial	Not Defined ^a	0.46	0.48	23.2
	+ Pitch-angle (Hiss)		0.48	0.69	18.9
	+ Pitch-angle (Chorus)		0.47	0.64	18.4
	+ Energy (Chorus)		0.54	0.75	19.1
	+ Mixed (Chorus)		0.51	0.74	18.1
1991/May Basic storm	Radial	Not Defined ^a	0.68	0.95	43.7
	+ Pitch-angle (Hiss)		0.44	0.60	31.9
	+ Pitch-angle (Chorus)		0.61	0.95	18.4
	+ Energy (Chorus)		0.00	0.00	31.7
	+ Mixed (Chorus)		0.00	0.48	29.1
1991/June Multi-dip storm	Radial	Not Defined ^a	0.61	0.80	18.0
	+ Pitch-angle (Hiss)		0.37	0.83	15.9
	+ Pitch-angle (Chorus)		0.29	0.81	15.8
	+ Energy (Chorus)		0.21	0.79	16.3
	+ Mixed (Chorus)		0.14	0.79	15.6
1991/July Basic storm	Radial	Not defined ^a	0.43	0.73	7.7
	+ Pitch-angle (Hiss)		0.39	0.84	8.6
	+ Pitch-angle (Chorus)		0.80	0.90	14.7
	+ Energy (Chorus)		0.83	0.67	8.1
	+ Mixed (Chorus)		0.71	0.66	8.5

Summary and Conclusion

- The 3-D VERB simulations show that during storm main phase and early recovery phase the estimated plasmopause is located near the inner edge of the outer belt so **pitch-angle scattering by chorus waves can be a dominant loss process in the outer belt.**
- We have also confirmed the important role played by **mixed energy and pitch-angle diffusion** by chorus waves, which tends to **reduce the fluxes enhanced by local acceleration**, resulting in the comparable level of the computed and measured fluxes.

Ongoing Project (KASI & UCLA) : Nowcasting of the Radiation Belt Environment

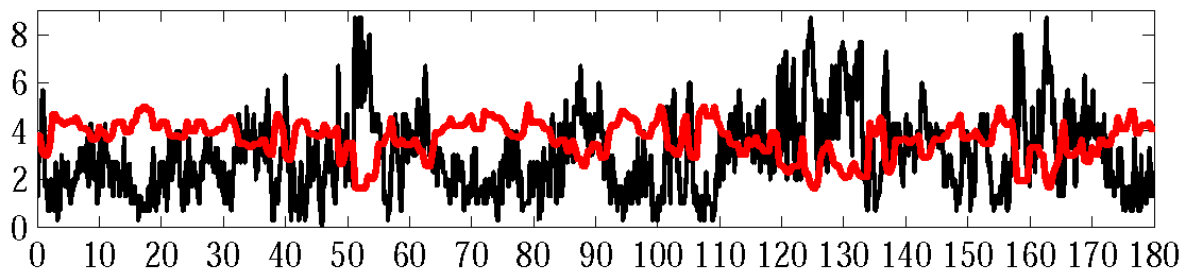


Backup slides

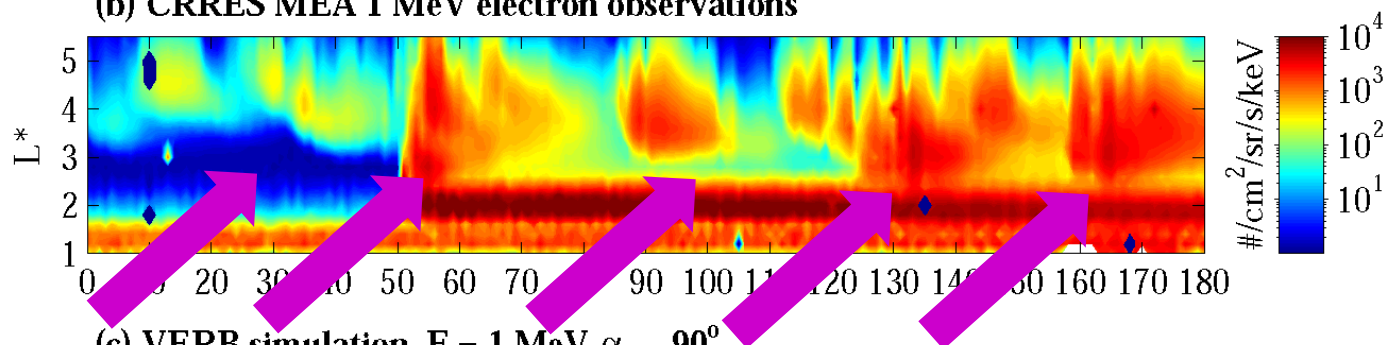
VERB Simulations

(2) Challenge interval: February 1, 1991 to July 31, 1991

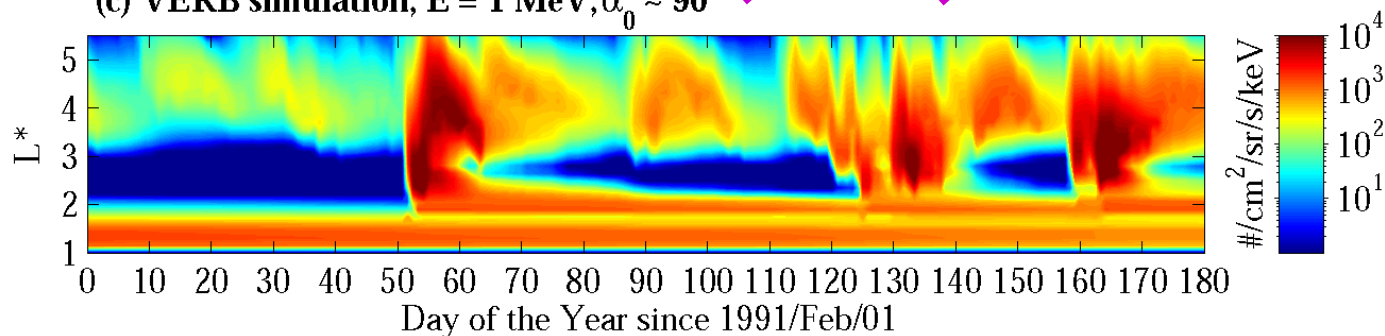
(a) Kp index and L_{pp}



(b) CRRES MEA 1 MeV electron observations



(c) VERB simulation, $E = 1 \text{ MeV}, \alpha_0 \sim 90^\circ$



Adopted Wave Parameters for Chorus Day-Night outside the Plasmapause

Type of Wave	Wave intensity B_w (pT)	λ_{\max}	Density model	MLT distribution of wave power (%)	Wave spectral properties	Wave propagation angle
Chorus Day	$10^{0.75+0.04\lambda}(2 \cdot 10^{0.73+0.91K_p/3319.2})^{0.5}$ $K_p \leq 2+$ $10^{0.75+0.04\lambda}(2 \cdot 10^{2.5+0.18K_p/3319.2})^{0.5}$ $2+ < K_p \leq 6$	35°	<i>Sheeley et al.</i> [2001]	25	$\omega_m/\Omega_e = 0.2$ $\delta\omega/\Omega_e = 0.1$	$\theta_m = 0^\circ$ $\delta\theta = 30^\circ$
Chorus Night	$50 \cdot (2 \cdot 10^{0.73+0.91K_p/3319.2})^{0.5}$ $K_p \leq 2+$ $50 \cdot (2 \cdot 10^{2.5+0.18K_p/3319.2})^{0.5}$ $2+ < K_p \leq 6$	15°	<i>Sheeley et al.</i> [2001]	25	$\omega_{uc}/\Omega_e = 0.3$ $\omega_{lc}/\Omega_e = 0.1$ $\omega_m/\Omega_e = 0.35$ $\delta\omega/\Omega_e = 0.15$	$\theta_{uc} = 45^\circ$ $\theta_{lc} = 0^\circ$ $\theta_m = 0^\circ$ $\delta\theta = 30^\circ$

The values of day and night chorus are based on works by *Horne et al.*, [2005], *Glauert and Horne* [2005], *Li et al.*, [2007], and *Shprits et al.*, [2009].

Adopted Wave Parameters for Plasmaspheric Hiss, Lightning-generated Whistlers, and VLF Transmitters (17.1 kHz and 22.3 kHz) inside the Plasmapause

Type of Wave	Plasmaspheric Hiss	Lightning-generated Whistlers	VLF transmitter 17.1 kHz	VLF transmitter 22.3 kHz
Wave intensity B_w (pT)	$80 \cdot K_p / 4$	$7 \cdot K_p / 4$	0.8pT	0.8pT
λ_{max}	45°			
Density model	<i>Carpenter and Andersen [1992] at L>2</i> <i>Starks et al. [2008] at L<2</i>			
MLT distribution of wave power (%)	60%	100%	2.4% each	2.4% each
Wave spectral properties (rad/s)	$\omega_m = 2\pi \cdot 550$ $\delta\omega = 2\pi \cdot 300$ $\omega_{uc} = 2\pi \cdot 2000$ $\omega_{lc} = 2\pi \cdot 100$	$\omega_m = 2\pi \cdot 4500$ $\delta\omega = 2\pi \cdot 2000$ $\omega_{uc} = 2\pi \cdot 6500$ $\omega_{lc} = 2\pi \cdot 2500$	$\omega_m = 2\pi \cdot 17100$ $\delta\omega = 2\pi \cdot 50$ $\omega_{uc} = 2\pi \cdot 17200$ $\omega_{lc} = 2\pi \cdot 17000$	$\omega_m = 2\pi \cdot 22300$ $\delta\omega = 2\pi \cdot 50$ $\omega_{uc} = 2\pi \cdot 22400$ $\omega_{lc} = 2\pi \cdot 22200$
Wave propagation angle	$\theta_m = 0^\circ, \delta\theta = 20^\circ$ $\theta_{uc} = 0^\circ, \theta_{lc} = 30^\circ$	$\theta_m = 45^\circ, \delta\theta = 22.5^\circ, \theta_{uc} = 67.5^\circ, \theta_{lc} = 22.5^\circ$		

Plasmaspheric hiss and lightning-generated whistler values are from *Meredith et al. [2007]*, and values for VLF transmitters are from *Abel and Thorne [1998]* and *Starks et al. [2008]*.

- Two points should be noticed about the adopted parameters.
 - (1) The wave power of the lightning-generated whistlers and plasmaspheric hiss. In this study, we have distinguished these two types of whistler mode waves simply by their frequencies rather than by their generation mechanisms.
 - (2) A recent study by *Starks et al.* [2008] reported that the intensity of VLF transmitters taken in a study of *Abel and Thorne* [1998] might be overestimated by a factor of approximately 10. For VLF transmitter waves in this study we used similar parameters as *Abel and Thorne* [1998] but scaled them by a factor of 10.
- Calculate the bounce-averaged diffusion coefficients by summing the contributions from the $|n| \leq 5$ cyclotron harmonic resonances in addition to the Landau resonance ($n = 0$).

Bounce-averaged diffusion coefficients

Chorus Day

Chorus Night

Plasmaspheric Hiss

Lightning-generated whistlers

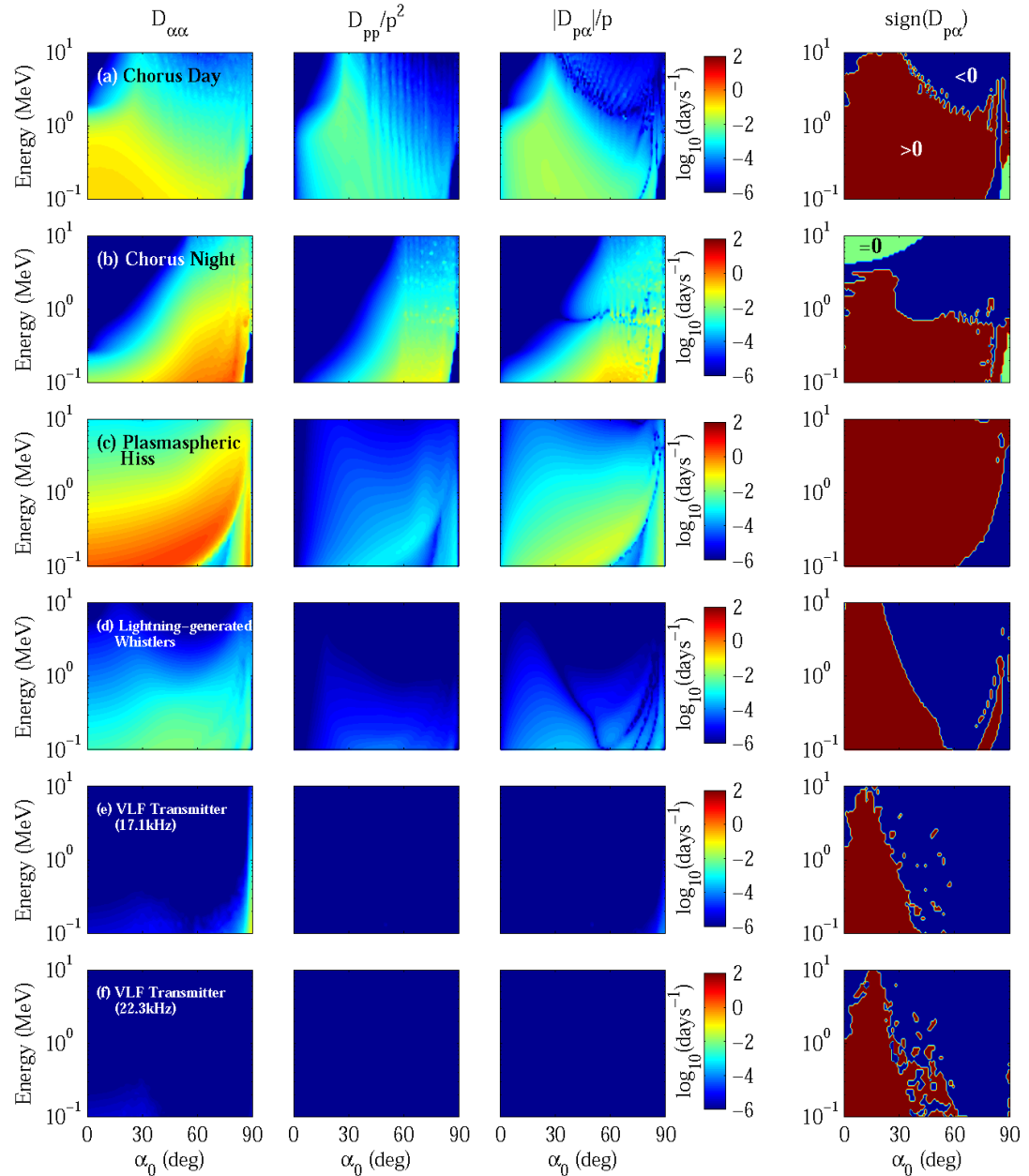
VLF Transmitter (17.1kHz)

VLF Transmitter (22.3kHz)

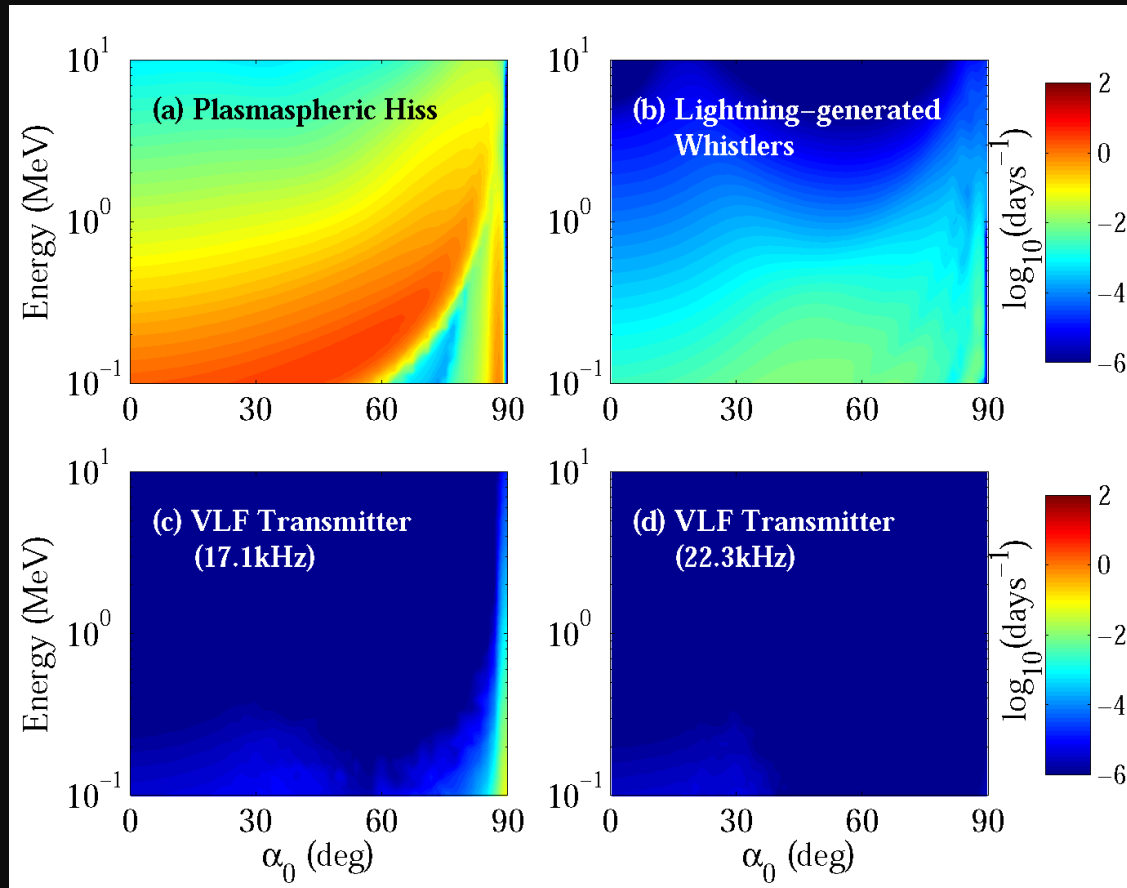
Pitch-angle diffusion

Momentum diffusion

Mixed diffusion



Bounce-averaged diffusion coefficients



- Pitch-angle scattering rates for the plasmaspheric hiss are significantly higher than those for the other types of waves.

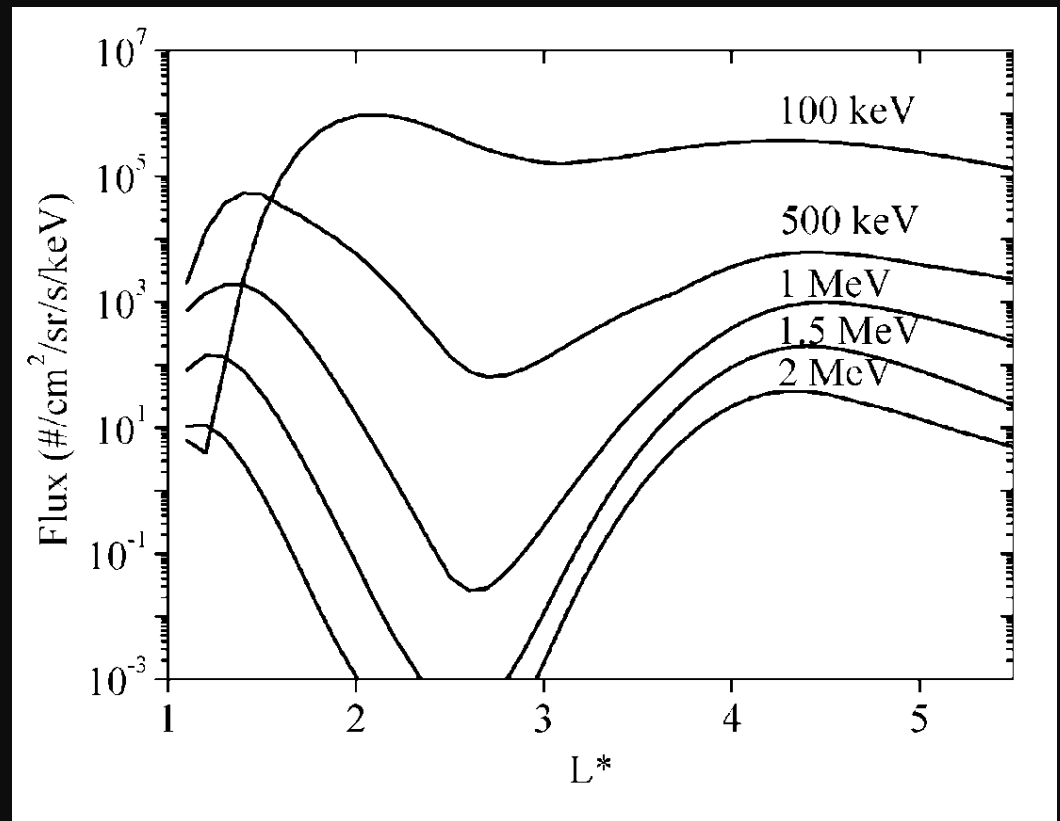
Boundary Conditions

Boundary	Conditions	Explanation
$L_{\min}^* = 1$	$f = 0$	Losses to the atmosphere
$L_{\max}^* = 5.5$	$f = f(t)$	CRRES observations
$\alpha_{\min} = 0.3^\circ$	$f = 0$	Empty loss cone in the weak diffusion regime
$\alpha_{\max} = 89.7^\circ$	$df/d\alpha = 0$	Flat pitch-angle distribution at 90°
$E_{\min} = 10 \text{ keV}$ at L_{\max}^*	$f = \text{constant}$	Balance of convective sources and losses
$E_{\max} = 10 \text{ MeV}$ at L_{\max}^*	$f = 0$	Absence of very high energy electrons

- Grid size : $31(L^*) \times 101(\text{pitch angle}) \times 101(\text{energy})$

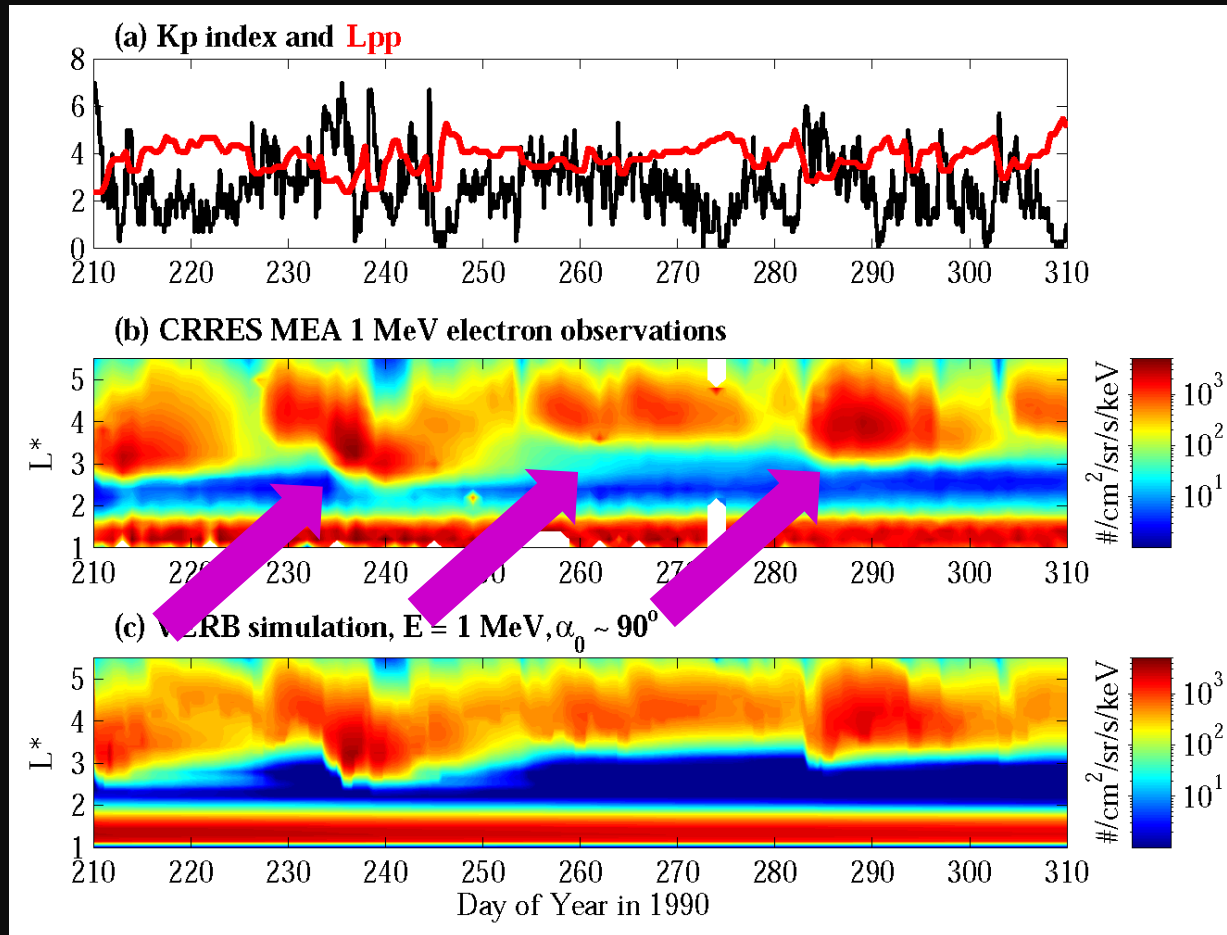
Initial Condition

- Use a steady state solution of the radial diffusion with $Kp=1$
- Will be taken from CRRES observations



VERB Simulations

(1) Training interval: August 15, 1990 to October 15, 1990



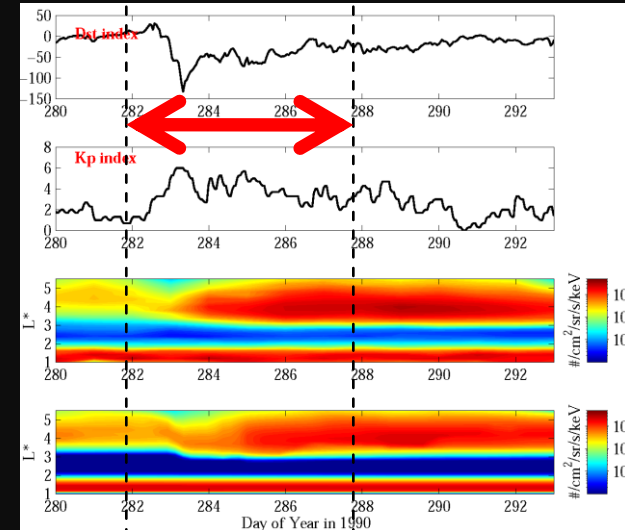
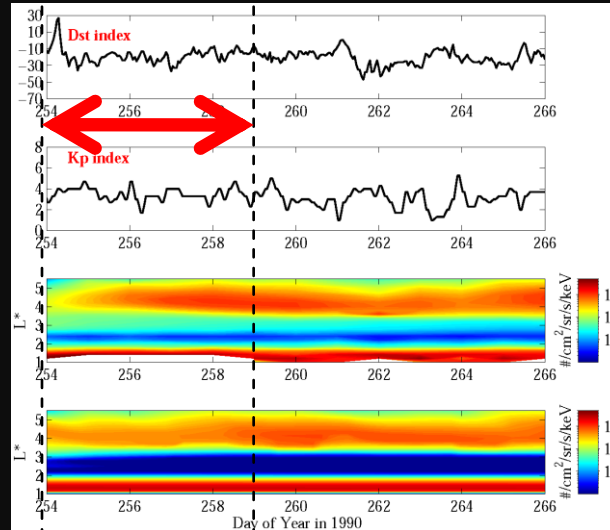
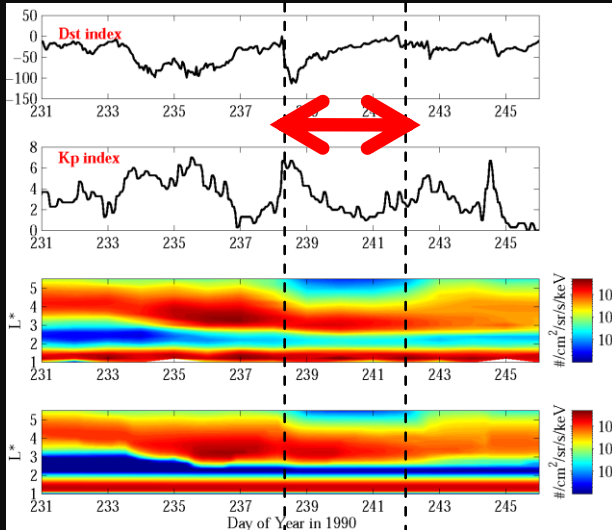
- The diffusion model predicts the instantaneous location of the upper boundary of the slot region, the empty slot region, and the stable inner belts, all of which show a good agreement with the CRRES observations.

August 26-30, 1990

(clear storm, preceded by another; $Dst_{min} \sim -100nT$)

October 9-15, 1990

(clear storm, $Dst_{min} \sim -120nT$)



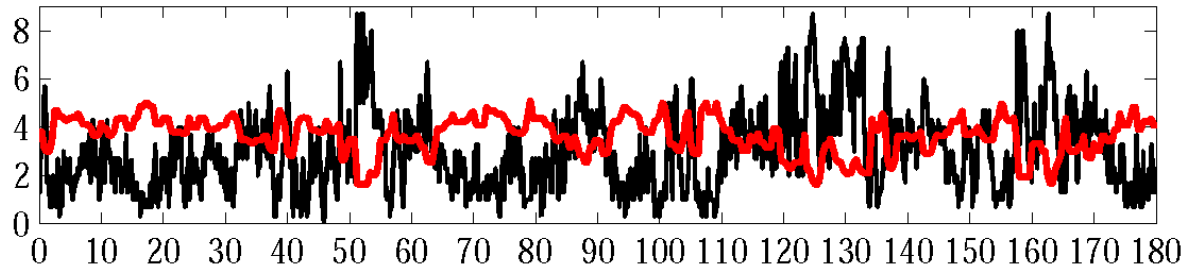
September 11-16, 1990

(“series of prolonged substorms”,
minimal Dst response)

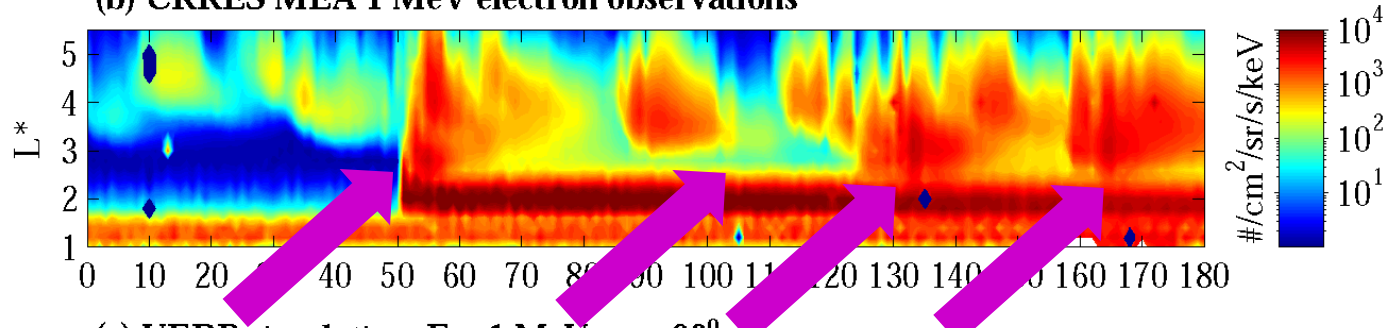
VERB Simulations

(2) Challenge interval: February 1, 1991 to July 31, 1991

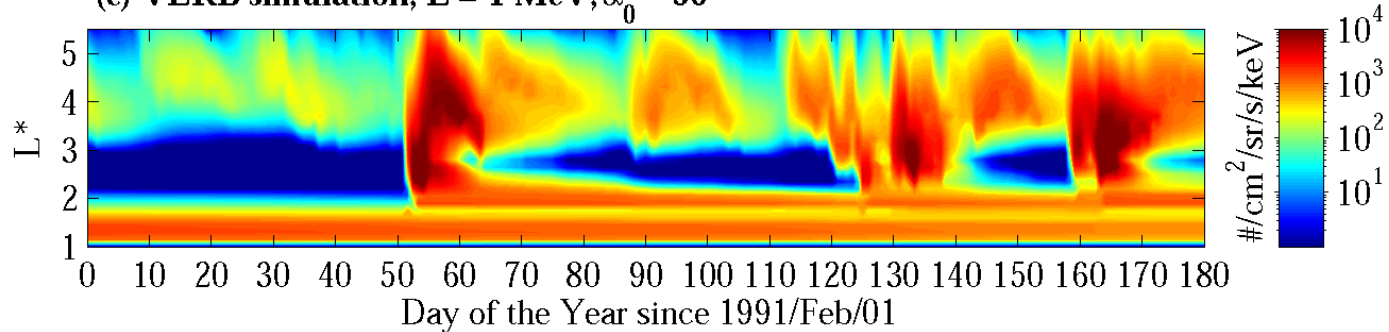
(a) Kp index and L_{pp}



(b) CRRES MEA 1 MeV electron observations

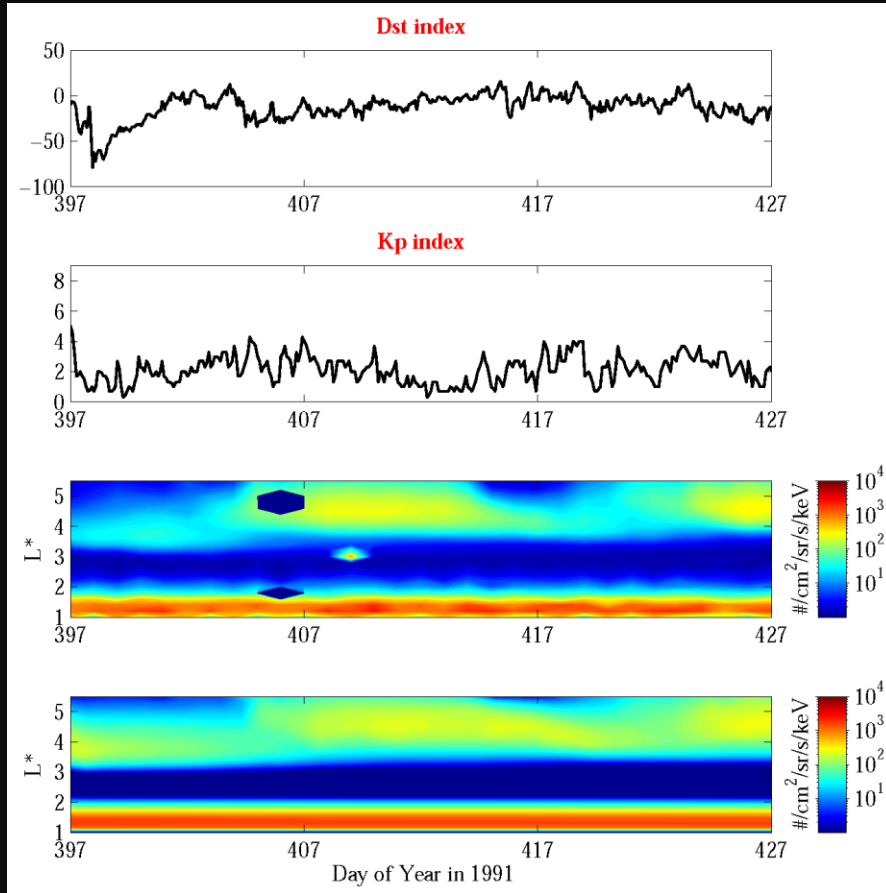


(c) VERB simulation, $E = 1 \text{ MeV}$, $\alpha_0 \sim 90^\circ$



February 1, 1991

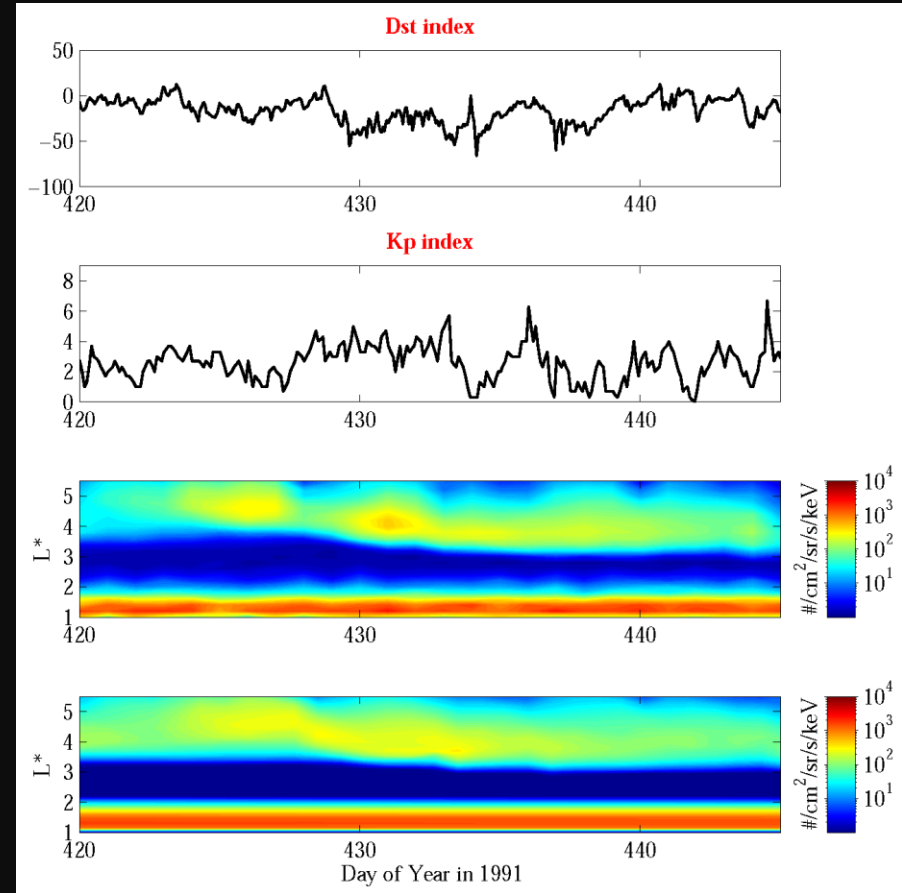
- $Dst_{\min} \sim -79$ nT
- Extended recovery phase



Feb. 1 Feb. 11 Feb. 21 Mar. 03

February 24, 1991

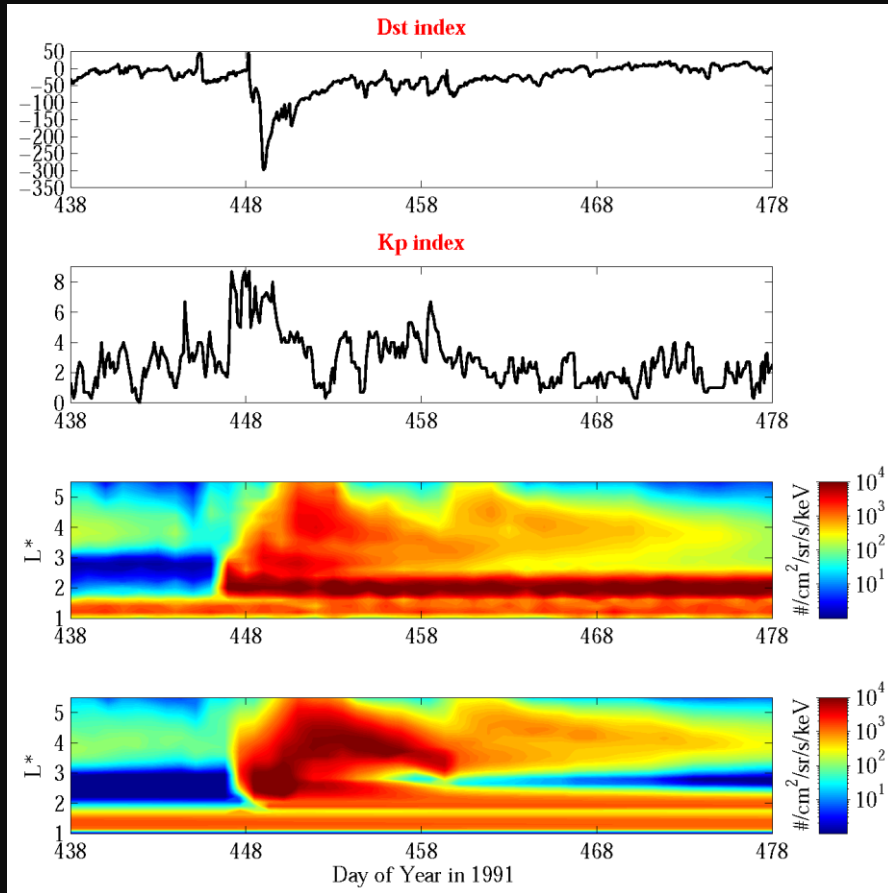
- Non-storm electron injection



Feb. 24 Mar. 6 Mar. 16

March 24, 1991

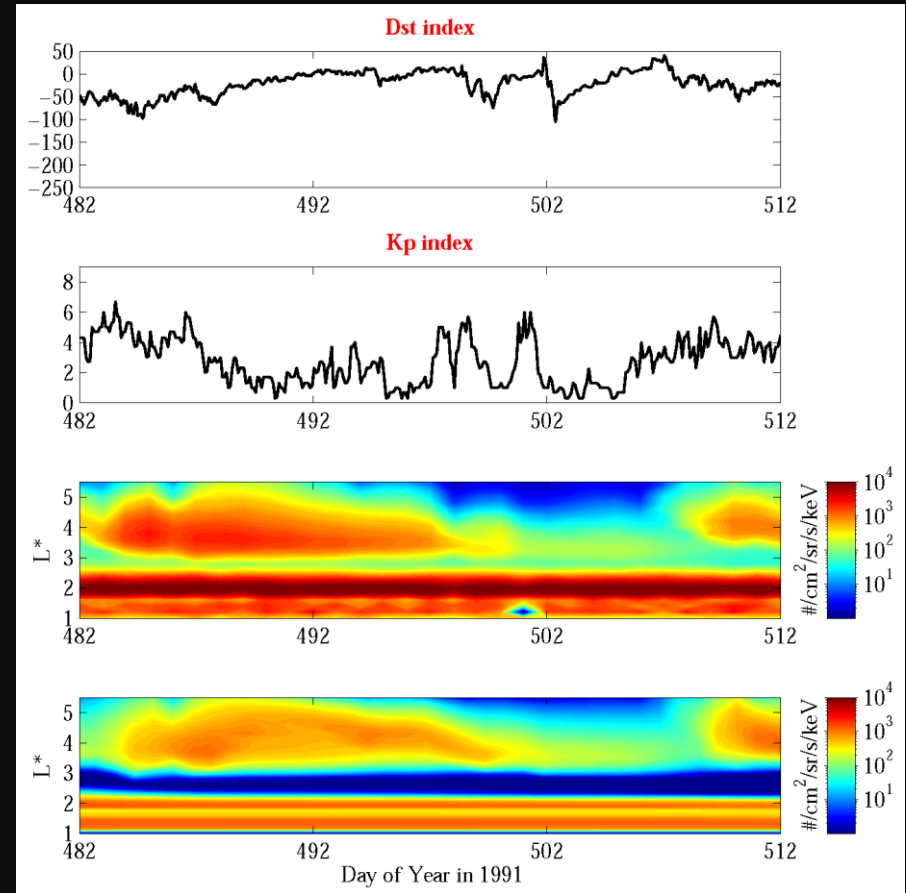
- Superstorm interval



Mar. 24

May 17, 1991

- Dst_{min} ~ -105 nT
- “classic” storm



May 17